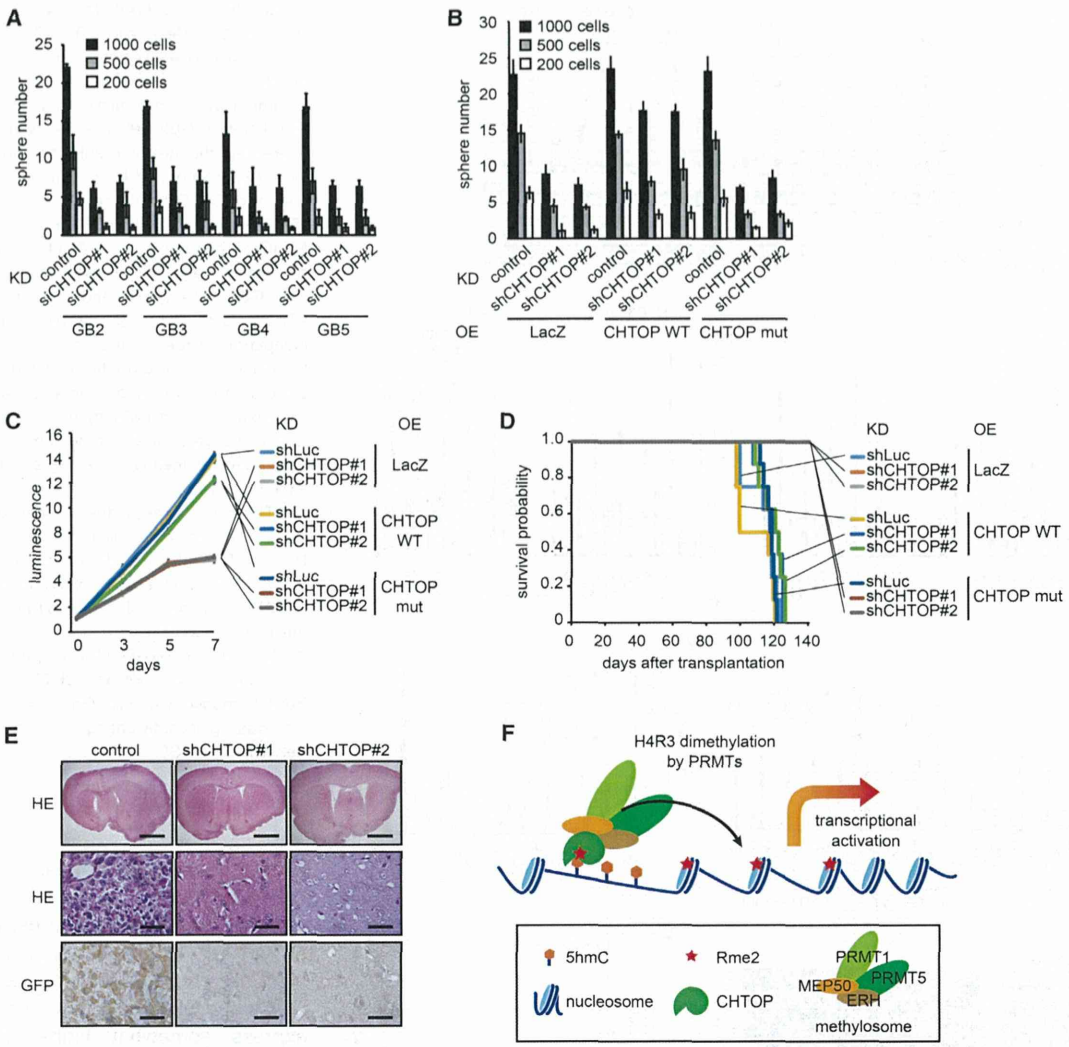

Figure 7. CHTOP Is Required for the Tumorigenicity of Glioblastoma Cells

(A) The number of spheres of glioblastoma cells transfected with siRNA targeting CHTOP. Data show the means ± SD of three independent experiments.

(B) The number of spheres of GB2 cells infected with a lentivirus expressing shRNA targeting CHTOP and/or a lentivirus expressing wild-type or mutant CHTOP. Data show the means ± SD of three independent experiments.

(C) Growth curves of GB2 cells infected with a lentivirus expressing shRNA targeting CHTOP and/or a lentivirus expressing wild-type or mutant CHTOP. Data show the means ± SD of three independent experiments.

(D) Kaplan-Meier survival curves of mice transplanted with 1.0×10^4 GB2 cells infected with a lentivirus expressing shRNA targeting CHTOP and/or a lentivirus expressing wild-type or mutant CHTOP.

(E) Histological examination of tumors developed in the mice in (D). At day 100, tissue sections were stained with HE or anti-GFP antibody. The scale bars represent 2 mm (upper panels) and 50 μm (lower panels).

(F) Schematic representation of 5hmC-mediated transcriptional activation. For details, see text.

See also Figure S6.

GB2~GB5 cells (Figures 7A and 7B) and GB2 cell proliferation (Figure 7C). These phenotypes were rescued by overexpression of wild-type CHTOP, but not by GAR mutant CHTOP. Mice receiving shCHTOP-expressing GB2 cells survived significantly longer than control mice (Figures 7D and 7E). Furthermore, we found that overexpression of CHTOP restored the tumorigenicity of shCHTOP-expressing GB2 cells (Figure 7D). These results suggest that 5hmC serves as a recruitment signal for the CHTOP-methylosome complex, which in turn methylates H4R3 and thereby activates the transcription of genes required for glioblastomagenesis (Figure 7F).

DISCUSSION

It is well known that glioblastomas contain genetic alterations in the p53, RB, and RTK pathways (Chen et al., 2012; Parsons

et al., 2008; Cancer Genome Atlas Research Network, 2008), as well as other genes, including the neurofibromatosis type 1 gene (Cancer Genome Atlas Research Network, 2008), the NF-κB inhibitor α gene (Bredel et al., 2011), and/or the IDH1 gene (Parsons et al., 2008). In the present study, we have shown that epigenetic alterations are also critical for the tumorigenicity of glioblastoma cells. We showed that proneural glioblastoma contains elevated levels of 5hmC and TET1 and that TET1-mediated production of 5hmC is required for glioblastomagenesis. We found that knockdown of TET1 in glioblastoma cells resulted in decreases in their proliferation, sphere formation, and tumorigenicity. Furthermore, we demonstrated that ectopic overexpression of wild-type, but not of a catalytically inactive mutant, TET1 restored the growth, sphere formation, and tumorigenicity, as well as 5hmC levels in glioblastoma cells in which TET1 had been knocked down.

Our results are in striking contrast to previous studies showing that 5hmC levels are markedly reduced in many tumor cells (Haffner et al., 2011; Kraus et al., 2012; Müller et al., 2012; Orr et al., 2012). This may be due to the differences in the culture conditions used and/or tumor subtypes. We cultured primary glioblastoma cells in serum-free conditions to retain their stem-cell-like properties and tumorigenicity. Indeed, our results showed that HeLa and U87MG cells cultured in the presence of serum contain extremely low levels of 5hmC.

Although most of previous studies did not consider subtypes of glioblastoma, Noushmehr et al. (2010) have reported that the IDH1 mutation is highly enriched in recurrent and secondary proneural glioblastoma and is strongly linked to the glioma-CpG island methylator phenotype (G-CIMP). Thus, secondary proneural glioblastomas are expected to have lower 5hmC levels. However, they have also reported that only a minor population of primary glioblastoma patients (<10%) display G-CIMP and IDH1 mutations. In this study, we focused on primary glioblastomas that can be cultured in serum-free media and found that most of the glioblastoma cell lines we established belong to the proneural subtype. Furthermore, we performed dot blot analysis of 5hmC using glioblastoma specimens of all subtypes and found that primary proneural glioblastomas that do not have an IDH1 mutation have markedly higher levels of 5hmC compared to other subtypes. We speculate that 5hmC may function differently at the molecular level in primary proneural glioblastoma compared to other subtypes of glioblastoma and other tumor cell types, and accordingly, 5hmC may recruit different molecules and elicit different downstream signals in proneural glioblastoma cells than it does in other tumor cells.

We have shown that 5hmC is not simply a demethylation intermediate but rather functions itself as an epigenetic mark modulating gene expression. Our results are consistent with previous findings showing that 5hmC is stably present in the genomes of ESCs and neuronal cells (Ficz et al., 2011; Guo et al., 2011; Hahn et al., 2013; Wu et al., 2011) and that enrichment of 5hmC is not necessarily associated with DNA demethylation (Hahn et al., 2013). Furthermore, Mbd3/NURD and MeCP2 have been reported to bind to both 5hmC and 5mC (Mellén et al., 2012; Yildirim et al., 2011). A systematic analysis of 5hmC-binding proteins using quantitative mass-spectrometry-based proteomics has identified a number of specific 5hmC-binding proteins (Spruijt et al., 2013). These reported results suggested that 5hmC, 5fC, and 5caC may recruit transcription regulators in certain cell types, as well as DNA repair proteins, which may also be involved in DNA demethylation. CHTOP was not identified in this latter study, presumably because this laboratory used mouse ESCs, mNPCs, and adult mouse brain tissue.

We found that TET1-mediated enrichment of 5hmC is critical for the expression of a number of cancer-related genes such as *EGFR*, *AKT3*, *CDK6*, *CCND2*, and *BRAF*. Furthermore, we found that CHTOP associated with 5hmC recruits the methylosome and that a component of the methylosome complex, PRMT1, methylates H4R3 and transactivates these genes. We investigated these genes because their products are key components of the RTK/RAS/PI(3)K- or the RB-signaling pathways and have been reported to be frequently altered in glioblastoma and play critical roles in glioblastomagenesis (Chen et al., 2012; Parsons et al., 2008; Cancer Genome Atlas Research Network, 2008). We would like to investigate whether hydroxymethylation of these five genes is necessary for the tumorigenicity of glioblastoma cells in future studies.

We found that TET1 knockdown in GB2 cells alters expression of many genes that do not have 5hmC peaks. It is possible that alterations in the expression of the genes that have 5hmC may affect that of other genes that do not have 5hmC. In addition, previous studies have shown that the TET family of proteins can interact with O-linked N-acetylglucosamine transferase (OGT) and function as a recruiter of OGT to chromatin (Chen et al., 2013; Deplus et al., 2013; Vella et al., 2013). We therefore speculate that TET1 has an important role that is independent of its catalytic activity.

Interestingly, we found that knockdown of CHTOP results in a reduction in global 5hmC levels in glioblastoma cells, whereas overexpression of CHTOP restores 5hmC levels. Thus, CHTOP may be required for maintaining 5hmC levels. For example, CHTOP may protect 5hmC from demethylation. Our results suggest that upregulation of CHTOP as well as TET1 may be responsible for the elevated levels of 5hmC observed in glioblastoma cells. We would like to investigate this issue in more detail in future studies. In addition, we found that hNPCs express somewhat lower levels of CHTOP than glioblastoma cells. It is therefore possible that reduced expression of CHTOP in hNPCs contributes, at least in part, to the poor expression of 5hmC, despite high TET1 expression in these cells.

Glioblastoma stem cells are subsets of glioblastoma cells that possess the capability of self-renewal and exhibit extensive tumorigenicity (Gilbertson and Rich, 2007; Lathia et al., 2011; Singh et al., 2004). Glioblastoma stem cells have been reported to be resistant to both chemotherapy and radiotherapy and thus are responsible for the poor prognosis of glioblastoma (Bao et al., 2006; Chen et al., 2012). In this study, we utilized glioblastoma cells cultured in serum-free medium, which enriches for glioblastoma stem cells (Lee et al., 2006). Thus, it is possible that 5hmC is critical for the tumorigenicity of glioblastoma stem cells. To test this possibility, we need to analyze the CD15- and/or CD133-positive stem cell population (Singh et al., 2004; Son et al., 2009). It also remains to be examined whether 5hmC is required specifically for glioblastoma stem cells or required for both glioblastoma stem and nonstem cells.

In conclusion, we found that 5hmC recruits the CHTOP-methylosome complex, which methylates H4R3 and transactivates cancer-related genes. Of particular interest is the fact that knockdown of TET1 as well as CHTOP results in the strong suppression of glioblastoma cell tumorigenicity. We therefore speculate that TET1 could be a promising molecular target for glioblastoma therapy. Because TET1-deficient mice are viable and fertile (Dawlaty et al., 2011, 2013), compounds targeting TET1 would be expected to have few serious side effects.

EXPERIMENTAL PROCEDURES

Antibodies

Antibodies used in immunoblot, ChIP, and (h)MeDIP assays are listed in Table S4.

Cell Culture

Following informed consent, tumor samples classified as primary glioblastoma were obtained from patients undergoing surgical treatment at the University of Tokyo Hospital, as approved by the Institutional Review Board. Mouse experiments were also approved by the Institutional Review Board. Tumors were washed and mechanically and enzymatically dissociated into single cells. Tumor cells were cultured in Dulbecco's modified Eagle's medium (DMEM)/F12 (Life Technologies) containing B27 supplement minus vitamin A (Life Technologies), epidermal growth factor, and fibroblast growth factor 2 (20 ng/ml each; Wako Pure Chemicals Industries). Fetal and ESC-derived hNPCs were purchased from Lonza and Millipore, respectively, and cultured under the same conditions. HEK293FT, HeLa, and human glioblastoma U87MG cells were cultured in DMEM (Nissui) containing 10% fetal bovine serum. GB2 cells transfected with siRNA targeting TET1 or control were seeded into a 96-well plate at the indicated cell number. The number of spheres was counted after 7 days. Cell viability was measured by CellTiter-Glo (Promega) according to the manufacturer's instructions.

RNAi

For lentivirus production, the lentiviral vector CS-Rfa-CG harboring an shRNA driven by the H1 promoter was transfected with the packaging vectors pCAG-HIV-gp and pCMV-VSV-G-RSV-Rev into HEK293FT cells using Lipofectamine 2000 Transfection Reagent (Life Technologies). All plasmids were kindly provided by H. Miyoshi (RIKEN BioResource Center). Virus supernatants were purified by ultracentrifugation at 25,000 rpm at 4°C for 90 min (SW28 rotor; Beckman Coulter Genomics). The target sequences for shRNAs are as follows: shTET1 no.1: 5′-GCATATTCCTTTGAAATAA-3′; shTET1 no. 2: 5′-GAACTAAACAAGATTAAGT-3′; shCHTOP no. 1: 5′-CTAAATGAGCGCTTTACTA-3′; shCHTOP no. 2: 5′-CCAAGATGTCTCTAAATGA-3′. The infection efficiency of the lentiviruses was more than 95%, as judged by GFP or Venus fluorescence. Transfection of Stealth siRNA duplexes targeting human TET1 (Life Technologies; catalog no. 10620318 and 10620319) or Silencer Select Pre-Designed siRNA targeting human CHTOP (Life Technologies; catalog no. s25092 and s25093) were performed using Lipofectamine RNAiMAX (Life Technologies) according to the manufacturer's instructions.

RNA Isolation and qRT-PCR

Total RNA was prepared by the NucleoSpin RNA Clean-up kit (Macherey-Nagel) and reverse transcribed with PrimeScript Reverse Transcriptase (TaKaRa). qPCR reactions were performed with Sybr Green I using a LightCycler480 (Roche Applied Science). The results were normalized with the detected values for TATA box-binding protein mRNA. Absolute mRNA levels of the TET family of genes were determined according to the standard curves generated by serial dilutions of plasmids containing TET1∼TET3. Primers used in qRT-PCR are shown in Table S5.

(h)MeDIP

Cells were digested with proteinase K and RNase A, and genomic DNA was purified by phenol/chloroform extraction. Purified genomic DNA was sonicated to 200–500 bp with a Handy Sonic (TOMY). (h)MeDIP was performed as described previously (Weber et al., 2005) with minor modifications. Briefly, 4 μg of fragmented genomic DNA was immunoprecipitated with 4 μl of polyclonal antibody against 5hmC (Active Motif) or 4 μg of monoclonal antibody against 5mC (Eurogentec) at 4°C overnight in a 500 μl of IP buffer (10 mM sodium phosphate [pH 7.0], 140 mM NaCl, and 0.05% Triton X-100). The mixture was incubated with 30 μl of Dynabeads Protein G at 4°C for 2 hr and washed three times with 1 ml of IP buffer. The beads were suspended in 20 μg of proteinase K and incubated at 55°C for at least 3 hr. Immunoprecipitated DNA was purified by phenol/chloroform extraction followed by isopropanol precipitation.

ACCESSION NUMBERS

Profiling and (h)MeDIP-seq data from this study are available from the Sequence Read Archive database (http://www.ncbi.nlm.nih.gov/sra) under the accession number SRP045590.

SUPPLEMENTAL INFORMATION

Supplemental Information includes Supplemental Experimental Procedures, six figures and five tables and can be found with this article online at http://dx.doi.org/10.1016/j.celrep.2014.08.071.

AUTHOR CONTRIBUTIONS

H.T. designed and performed most of the experiments. T. Sato performed dot blot analysis. R.K.-N. and Y.N.-N. established glioblastoma cell lines and discussed the results. K.M., Y.K., and K.S. performed sequence analysis and analyzed the bioinformatic data. H.O. and C.T. supervised the production of recombinant CHTOP. Y.M. performed immunohistochemical analysis of glioblastoma specimens. Y.S., Takeo Suzuki, Tsutomu Suzuki, H.K.-H., and M.O. performed mass spectrometric analysis. T.T., Y.I., A.M., and N.S. prepared glioblastoma specimens. H.T. and T.A. wrote the paper.

ACKNOWLEDGMENTS

This work was supported by Research Program of Innovative Cell Biology by Innovative Technology (Integrated Systems Analysis of Cellular Oncogenic Signaling Networks), Grants-in-Aid for Scientific Research on Innovative Areas (Integrative Research on Cancer Microenvironment Network), Project for Development of Innovative Research on Cancer Therapeutics, Takeda Science Foundation, and in part by Global COE Program (Integrative Life Science Based on the Study of Biosignaling Mechanisms), MEXT, Japan.

Received: April 5, 2014
Revised: July 29, 2014
Accepted: August 27, 2014
Published: October 2, 2014

REFERENCES

Bao, S., Wu, Q., McLendon, R.E., Hao, Y., Shi, Q., Hjelmeland, A.B., Dewhirst, M.W., Bigner, D.D., and Rich, J.N. (2006). Glioma stem cells promote radioresistance by preferential activation of the DNA damage response. Nature *444*, 756–760.

Baylin, S.B., and Jones, P.A. (2011). A decade of exploring the cancer epigenome - biological and translational implications. Nat. Rev. Cancer *11*, 726–734.

Bedford, M.T., and Clarke, S.G. (2009). Protein arginine methylation in mammals: who, what, and why. Mol. Cell *33*, 1–13.

Bird, A. (2001). Molecular biology. Methylation talk between histones and DNA. Science *294*, 2113–2115.

Bredel, M., Scholtens, D.M., Yadav, A.K., Alvarez, A.A., Renfrow, J.J., Chandler, J.P., Yu, I.L., Carro, M.S., Dai, F., Tagge, M.J., et al. (2011). NFKBIA deletion in glioblastomas. N. Engl. J. Med. *364*, 627–637.

Cancer Genome Atlas Research Network (2008). Comprehensive genomic characterization defines human glioblastoma genes and core pathways. Nature *455*, 1061–1068.

Chen, J., Li, Y., Yu, T.S., McKay, R.M., Burns, D.K., Kernie, S.G., and Parada, L.F. (2012). A restricted cell population propagates glioblastoma growth after chemotherapy. Nature *488*, 522–526.

Chen, Q., Chen, Y., Bian, C., Fujiki, R., and Yu, X. (2013). TET2 promotes histone O-GlcNAcylation during gene transcription. Nature *493*, 561–564.

Cimmino, L., Abdel-Wahab, O., Levine, R.L., and Aifantis, I. (2011). TET family proteins and their role in stem cell differentiation and transformation. Cell Stem Cell *9*, 193–204.

Dang, L., White, D.W., Gross, S., Bennett, B.D., Bittinger, M.A., Driggers, E.M., Fantin, V.R., Jang, H.G., Jin, S., Keenan, M.C., et al. (2009). Cancer-associated IDH1 mutations produce 2-hydroxyglutarate. Nature *462*, 739–744.

Dawlaty, M.M., Ganz, K., Powell, B.E., Hu, Y.C., Markoulaki, S., Cheng, A.W., Gao, Q., Kim, J., Choi, S.W., Page, D.C., and Jaenisch, R. (2011). Tet1 is dispensable for maintaining pluripotency and its loss is compatible with embryonic and postnatal development. Cell Stem Cell *9*, 166–175.

Dawlaty, M.M., Breiling, A., Le, T., Raddatz, G., Barrasa, M.I., Cheng, A.W., Gao, Q., Powell, B.E., Li, Z., Xu, M., et al. (2013). Combined deficiency of Tet1 and Tet2 causes epigenetic abnormalities but is compatible with postnatal development. Dev. Cell *24*, 310–323.

Delhommeau, F., Dupont, S., Della Valle, V., James, C., Trannoy, S., Massé, A., Kosmider, O., Le Couedic, J.P., Robert, F., Alberdi, A., et al. (2009). Mutation in TET2 in myeloid cancers. N. Engl. J. Med. *360*, 2289–2301.

Deplus, R., Delatte, B., Schwinn, M.K., Defrance, M., Méndez, J., Murphy, N., Dawson, M.A., Volkmar, M., Putmans, P., Calonne, E., et al. (2013). TET2 and TET3 regulate GlcNAcylation and H3K4 methylation through OGT and SET1/COMPASS. EMBO J. *32*, 645–655.

Ficz, G., Branco, M.R., Seisenberger, S., Santos, F., Krueger, F., Hore, T.A., Marques, C.J., Andrews, S., and Reik, W. (2011). Dynamic regulation of 5-hydroxymethylcytosine in mouse ES cells and during differentiation. Nature *473*, 398–402.

Figueroa, M.E., Abdel-Wahab, O., Lu, C., Ward, P.S., Patel, J., Shih, A., Li, Y., Bhagwat, N., Vasanthakumar, A., Fernandez, H.F., et al. (2010). Leukemic IDH1 and IDH2 mutations result in a hypermethylation phenotype, disrupt TET2 function, and impair hematopoietic differentiation. Cancer Cell *18*, 553–567.

Friesen, W.J., Paushkin, S., Wyce, A., Massenet, S., Pesiridis, G.S., Van Duyne, G., Rappsilber, J., Mann, M., and Dreyfuss, G. (2001). The methylosome, a 20S complex containing JBP1 and pICln, produces dimethylarginine-modified Sm proteins. Mol. Cell. Biol. *21*, 8289–8300.

Furnari, F.B., Fenton, T., Bachoo, R.M., Mukasa, A., Stommel, J.M., Stegh, A., Hahn, W.C., Ligon, K.L., Louis, D.N., Brennan, C., et al. (2007). Malignant astrocytic glioma: genetics, biology, and paths to treatment. Genes Dev. *21*, 2683–2710.

Gilbertson, R.J., and Rich, J.N. (2007). Making a tumour's bed: glioblastoma stem cells and the vascular niche. Nat. Rev. Cancer *7*, 733–736.

Goldberg, A.D., Allis, C.D., and Bernstein, E. (2007). Epigenetics: a landscape takes shape. Cell *128*, 635–638.

Guo, J.U., Su, Y., Zhong, C., Ming, G.L., and Song, H. (2011). Hydroxylation of 5-methylcytosine by TET1 promotes active DNA demethylation in the adult brain. Cell *145*, 423–434.

Haffner, M.C., Chaux, A., Meeker, A.K., Esopi, D.M., Gerber, J., Pellakuru, L.G., Toubaji, A., Argani, P., Iacobuzio-Donahue, C., Nelson, W.G., et al. (2011). Global 5-hydroxymethylcytosine content is significantly reduced in tissue stem/progenitor cell compartments and in human cancers. Oncotarget *2*, 627–637.

Hahn, M.A., Qiu, R., Wu, X., Li, A.X., Zhang, H., Wang, J., Jui, J., Jin, S.G., Jiang, Y., Pfeifer, G.P., and Lu, Q. (2013). Dynamics of 5-hydroxymethylcytosine and chromatin marks in mammalian neurogenesis. Cell Rep. *3*, 291–300.

He, Y.F., Li, B.Z., Li, Z., Liu, P., Wang, Y., Tang, Q., Ding, J., Jia, Y., Chen, Z., Li, L., et al. (2011). Tet-mediated formation of 5-carboxylcytosine and its excision by TDG in mammalian DNA. Science *333*, 1303–1307.

Hsu, C.H., Peng, K.L., Kang, M.L., Chen, Y.R., Yang, Y.C., Tsai, C.H., Chu, C.S., Jeng, Y.M., Chen, Y.T., Lin, F.M., et al. (2012). TET1 suppresses cancer invasion by activating the tissue inhibitors of metalloproteinases. Cell Rep. *2*, 568–579.

Huang, S., Litt, M., and Felsenfeld, G. (2005). Methylation of histone H4 by arginine methyltransferase PRMT1 is essential in vivo for many subsequent histone modifications. Genes Dev. *19*, 1885–1893.

Ito, S., Shen, L., Dai, Q., Wu, S.C., Collins, L.B., Swenberg, J.A., He, C., and Zhang, Y. (2011). Tet proteins can convert 5-methylcytosine to 5-formylcytosine and 5-carboxylcytosine. Science *333*, 1300–1303.

Jones, P.A. (2012). Functions of DNA methylation: islands, start sites, gene bodies and beyond. Nat. Rev. Genet. *13*, 484–492.

Koh, K.P., Yabuuchi, A., Rao, S., Huang, Y., Cunniff, K., Nardone, J., Laiho, A., Tahiliani, M., Sommer, C.A., Mostoslavsky, G., et al. (2011). Tet1 and Tet2 regulate 5-hydroxymethylcytosine production and cell lineage specification in mouse embryonic stem cells. Cell Stem Cell *8*, 200–213.

Koyama-Nasu, R., Nasu-Nishimura, Y., Todo, T., Ino, Y., Saito, N., Aburatani, H., Funato, K., Echizen, K., Sugano, H., Haruta, R., et al. (2013). The critical role of cyclin D2 in cell cycle progression and tumorigenicity of glioblastoma stem cells. Oncogene *32*, 3840–3845.

Kraus, T.F., Globisch, D., Wagner, M., Eigenbrod, S., Widmann, D., Münzel, M., Müller, M., Pfaffeneder, T., Hackner, B., Feiden, W., et al. (2012). Low values of 5-hydroxymethylcytosine (5hmC), the "sixth base," are associated with anaplasia in human brain tumors. Int. J. Cancer *131*, 1577–1590.

Lathia, J.D., Heddleston, J.M., Venere, M., and Rich, J.N. (2011). Deadly teamwork: neural cancer stem cells and the tumor microenvironment. Cell Stem Cell *8*, 482–485.

Lee, J., Kotliarova, S., Kotliarov, Y., Li, A., Su, Q., Donin, N.M., Pastorino, S., Purow, B.W., Christopher, N., Zhang, W., et al. (2006). Tumor stem cells derived from glioblastomas cultured in bFGF and EGF more closely mirror the phenotype and genotype of primary tumors than do serum-cultured cell lines. Cancer Cell *9*, 391–403.

Lian, C.G., Xu, Y., Ceol, C., Wu, F., Larson, A., Dresser, K., Xu, W., Tan, L., Hu, Y., Zhan, Q., et al. (2012). Loss of 5-hydroxymethylcytosine is an epigenetic hallmark of melanoma. Cell *150*, 1135–1146.

Lottaz, C., Beier, D., Meyer, K., Kumar, P., Hermann, A., Schwarz, J., Junker, M., Oefner, P.J., Bogdahn, U., Wischhusen, J., et al. (2010). Transcriptional profiles of CD133+ and CD133- glioblastoma-derived cancer stem cell lines suggest different cells of origin. Cancer Res. *70*, 2030–2040.

Martin, C., and Zhang, Y. (2005). The diverse functions of histone lysine methylation. Nat. Rev. Mol. Cell Biol. *6*, 838–849.

Mellén, M., Ayata, P., Dewell, S., Kriaucionis, S., and Heintz, N. (2012). MeCP2 binds to 5hmC enriched within active genes and accessible chromatin in the nervous system. Cell *151*, 1417–1430.

Meshorer, E., Yellajoshula, D., George, E., Scambler, P.J., Brown, D.T., and Misteli, T. (2006). Hyperdynamic plasticity of chromatin proteins in pluripotent embryonic stem cells. Dev. Cell *10*, 105–116.

Müller, T., Gessi, M., Waha, A., Isselstein, L.J., Luxen, D., Freihoff, D., Freihoff, J., Becker, A., Simon, M., Hammes, J., et al. (2012). Nuclear exclusion of TET1 is associated with loss of 5-hydroxymethylcytosine in IDH1 wild-type gliomas. Am. J. Pathol. *181*, 675–683.

Noushmehr, H., Weisenberger, D.J., Diefes, K., Phillips, H.S., Pujara, K., Berman, B.P., Pan, F., Pelloski, C.E., Sulman, E.P., Bhat, K.P., et al. (2010). Identification of a CpG island methylator phenotype that defines a distinct subgroup of glioma. Cancer Cell *17*, 510–522.

Ono, R., Taki, T., Taketani, T., Taniwaki, M., Kobayashi, H., and Hayashi, Y. (2002). LCX, leukemia-associated protein with a CXXC domain, is fused to MLL in acute myeloid leukemia with trilineage dysplasia having t(10;11)(q22;q23). Cancer Res. *62*, 4075–4080.

Orr, B.A., Haffner, M.C., Nelson, W.G., Yegnasubramanian, S., and Eberhart, C.G. (2012). Decreased 5-hydroxymethylcytosine is associated with neural progenitor phenotype in normal brain and shorter survival in malignant glioma. PLoS ONE *7*, e41036.

Parsons, D.W., Jones, S., Zhang, X., Lin, J.C., Leary, R.J., Angenendt, P., Mankoo, P., Carter, H., Siu, I.M., Gallia, G.L., et al. (2008). An integrated genomic analysis of human glioblastoma multiforme. Science *321*, 1807–1812.

Rajyaguru, P., and Parker, R. (2012). RGG motif proteins: modulators of mRNA functional states. Cell Cycle *11*, 2594–2599.

Sasaki, H., and Matsui, Y. (2008). Epigenetic events in mammalian germ-cell development: reprogramming and beyond. Nat. Rev. Genet. *9*, 129–140.

Shen, L., Song, C.X., He, C., and Zhang, Y. (2014). Mechanism and function of oxidative reversal of DNA and RNA methylation. Annu. Rev. Biochem. *83*, 585–614.

Singh, S.K., Hawkins, C., Clarke, I.D., Squire, J.A., Bayani, J., Hide, T., Henkelman, R.M., Cusimano, M.D., and Dirks, P.B. (2004). Identification of human brain tumour initiating cells. Nature *432*, 396–401.

Son, M.J., Woolard, K., Nam, D.H., Lee, J., and Fine, H.A. (2009). SSEA-1 is an enrichment marker for tumor-initiating cells in human glioblastoma. Cell Stem Cell *4*, 440–452.

Spruijt, C.G., Gnerlich, F., Smits, A.H., Pfaffeneder, T., Jansen, P.W., Bauer, C., Münzel, M., Wagner, M., Müller, M., Khan, F., et al. (2013). Dynamic readers for 5-(hydroxy)methylcytosine and its oxidized derivatives. Cell *152*, 1146–1159.

Stupp, R., Mason, W.P., van den Bent, M.J., Weller, M., Fisher, B., Taphoorn, M.J., Belanger, K., Brandes, A.A., Marosi, C., Bogdahn, U., et al.; European Organisation for Research and Treatment of Cancer Brain Tumor and Radiotherapy Groups; National Cancer Institute of Canada Clinical Trials Group (2005). Radiotherapy plus concomitant and adjuvant temozolomide for glioblastoma. N. Engl. J. Med. *352*, 987–996.

Tahiliani, M., Koh, K.P., Shen, Y., Pastor, W.A., Bandukwala, H., Brudno, Y., Agarwal, S., Iyer, L.M., Liu, D.R., Aravind, L., and Rao, A. (2009). Conversion of 5-methylcytosine to 5-hydroxymethylcytosine in mammalian DNA by MLL partner TET1. Science *324*, 930–935.

van Dijk, T.B., Gillemans, N., Stein, C., Fanis, P., Demmers, J., van de Corput, M., Essers, J., Grosveld, F., Bauer, U.M., and Philipsen, S. (2010). Friend of Prmt1, a novel chromatin target of protein arginine methyltransferases. Mol. Cell. Biol. *30*, 260–272.

Vella, P., Scelfo, A., Jammula, S., Chiacchiera, F., Williams, K., Cuomo, A., Roberto, A., Christensen, J., Bonaldi, T., Helin, K., and Pasini, D. (2013). Tet proteins connect the O-linked N-acetylglucosamine transferase Ogt to chromatin in embryonic stem cells. Mol. Cell *49*, 645–656.

Wang, H., Huang, Z.Q., Xia, L., Feng, Q., Erdjument-Bromage, H., Strahl, B.D., Briggs, S.D., Allis, C.D., Wong, J., Tempst, P., and Zhang, Y. (2001). Methylation of histone H4 at arginine 3 facilitating transcriptional activation by nuclear hormone receptor. Science *293*, 853–857.

Ward, P.S., Patel, J., Wise, D.R., Abdel-Wahab, O., Bennett, B.D., Coller, H.A., Cross, J.R., Fantin, V.R., Hedvat, C.V., Perl, A.E., et al. (2010). The common feature of leukemia-associated IDH1 and IDH2 mutations is a neomorphic enzyme activity converting alpha-ketoglutarate to 2-hydroxyglutarate. Cancer Cell *17*, 225–234.

Weber, M., Davies, J.J., Wittig, D., Oakeley, E.J., Haase, M., Lam, W.L., and Schübeler, D. (2005). Chromosome-wide and promoter-specific analyses identify sites of differential DNA methylation in normal and transformed human cells. Nat. Genet. *37*, 853–862.

Wu, H., and Zhang, Y. (2014). Reversing DNA methylation: mechanisms, genomics, and biological functions. Cell *156*, 45–68.

Wu, H., D'Alessio, A.C., Ito, S., Wang, Z., Cui, K., Zhao, K., Sun, Y.E., and Zhang, Y. (2011). Genome-wide analysis of 5-hydroxymethylcytosine distribution reveals its dual function in transcriptional regulation in mouse embryonic stem cells. Genes Dev. *25*, 679–684.

Xu, W., Yang, H., Liu, Y., Yang, Y., Wang, P., Kim, S.H., Ito, S., Yang, C., Wang, P., Xiao, M.T., et al. (2011). Oncometabolite 2-hydroxyglutarate is a competitive inhibitor of α-ketoglutarate-dependent dioxygenases. Cancer Cell *19*, 17–30.

Yildirim, O., Li, R., Hung, J.H., Chen, P.B., Dong, X., Ee, L.S., Weng, Z., Rando, O.J., and Fazzio, T.G. (2011). Mbd3/NURD complex regulates expression of 5-hydroxymethylcytosine marked genes in embryonic stem cells. Cell *147*, 1498–1510.

Zullo, A.J., Michaud, M., Zhang, W., and Grusby, M.J. (2009). Identification of the small protein rich in arginine and glycine (SRAG): a newly identified nucleolar protein that can regulate cell proliferation. J. Biol. Chem. *284*, 12504–12511.

J Neurooncol (2015) 121:239–250
DOI 10.1007/s11060-014-1630-z

LABORATORY INVESTIGATION

Strong therapeutic potential of γ-secretase inhibitor MRK003 for CD44-high and CD133-low glioblastoma initiating cells

Shingo Tanaka · Mitsutoshi Nakada · Daisuke Yamada · Ichiro Nakano · Tomoki Todo · Yasushi Ino · Takayuki Hoshii · Yuko Tadokoro · Kumiko Ohta · Mohamed A. E. Ali · Yutaka Hayashi · Jun-ichiro Hamada · Atsushi Hirao

Received: 13 May 2014 / Accepted: 1 October 2014 / Published online: 8 October 2014

Abstract The Notch signal regulates both cell viability and apoptosis, and maintains stemness of various cancers including glioblastoma (GBM). Although Notch signal inhibition may be an effective strategy in treating GBM initiating cells (GICs), its applicability to the different subtypes of GBM remains unclear. Here, we analyzed the effectiveness of MRK003, a preclinical γ-secretase inhibitor, on GICs. Nine patient-derived GICs were treated by MRK003, and its efficacy on cell viability, apoptosis, sphere forming ability and Akt expression level which might be related to Notch downstream and be greatly important signals in GBM was evaluated. MRK003 suppressed viability and sphere-formation ability, and induced apoptosis in all GICs in varying doses of MRK003. Based on their sensitivities to MRK003, the nine GICs were divided into "relatively sensitive" and "relatively resistant" GICs. Sensitivity to MRK003 was associated with its inhibitory effect on Akt pathway. Transgenic expression of the myristoylated Akt vector in relatively sensitive GICs partially rescued the effect of MRK003, suggesting that the effect of MRK003 was, at least in part, mediated through inhibition of the Akt pathway. These GICs were differentiated by the expression of CD44 and CD133 with flow cytometric analysis. The relatively sensitive GICs are CD44-high and CD133-low. The IC_{50} of MRK003 in a set of GICs exhibited a negative correlation with CD44 and positive correlation with CD133. Collectively, MRK003 is partially mediated by the Akt pathway and has strong therapeutic potential for CD44-high and CD133-low GICs.

Keywords Glioma · MRK003 · GBM initiating cells · CD44 · CD133

Introduction

Glioblastoma (GBM) is the most malignant primary brain tumor in humans. Despite the momentous progress in surgical and neuro-radiological techniques, the median overall survival period of GBM patients is from 14.6 to 16.0 months post diagnosis without major improvement for decades [1–4]. GBM is characterized by a heterogeneous population of tumor cells, exhibiting high invasive ability and chemo- and radio-resistance [2]. Accumulated evidence has suggested that tumor initiation is caused by a small fraction of tumor cell termed GBM initiating cells (GICs) [5, 6]. The significance of targeting GICs may be important for successful treatment of GBM [7, 8].

The Notch signals play a variety of roles in cancer initiation and propagation, and are critical for maintenance of stemness [9]. This pathway is mediated by cell–cell contact, thereby initiating the binding of a ligand to a Notch

Electronic supplementary material The online version of this article (doi:10.1007/s11060-014-1630-z) contains supplementary material, which is available to authorized users.

S. Tanaka · M. Nakada (✉) · Y. Hayashi · J. Hamada
Department of Neurosurgery, Division of Neuroscience, Graduate School of Medical Science, Kanazawa University, 13-1 Takara-machi, Kanazawa, Ishikawa 920-8641, Japan
e-mail: mnakada@med.kanazawa-u.ac.jp

S. Tanaka · D. Yamada · T. Hoshii · Y. Tadokoro · K. Ohta · M. A. E. Ali · A. Hirao
Division of Molecular Genetics, Cancer Research Institute, Kanazawa University, Kanazawa, Japan

I. Nakano
Department of Neurological Surgery, The Ohio State University, Columbus, OH, USA

T. Todo · Y. Ino
Division of Innovative Cancer Therapy, The Institute of Medical Science, The University of Tokyo, Hongo, Japan

receptor with subsequent activation of the intracellular signaling events. Upon binding of ligand, Notch intracellular domain (NICD) is released by γ-secretase, which then translocates to the nucleus, interacts with the specific transcriptional factors, and subsequently activates downstream target genes [9, 10]. The activation of Notch signaling was identified in a variety of cancers, including GBM [10–15]. Notch displays intense crosstalk with other oncogenic pathways, including phosphoinositide 3-kinase (PI3K)/Akt pathway that is a major pathway in GBM [16], Janus-activated kinase (JAK)/STAT pathway, Sonic hedgehog pathway and Wnt pathway [10, 17–21]. Hence, suppression of the Notch signal inhibition may offer an ideal strategy for the treatment of multiple types of cancers.

MRK003 is expected as a novel Notch inhibitor, and is known to be the most effective small molecule inhibitors amongst several other Notch inhibitors [22]. Data obtained with pre-clinical studies for pancreatic carcinoma, breast cancer, and T cell lymphoblastic leukemia demonstrated that MRK003 significantly suppressed cell proliferation and induced apoptosis in vivo [23–27]. Recent studies including ours have suggested that MRK003 suppresses both proliferation and invasion of GBM cell lines [19–21, 28]. In addition, MRK003 suppressed tumor growth and tumor initiation capacity in two GBM neurosphere lines [29]. Saito et al. revealed that Notch inhibition demonstrated good response at rate of 43.9 % for proneural subtype of GBM [30]. However, study with patient-derived GICs treated by MRK003 has never been reported.

In this study, we performed a set of in vitro assays including cell viability assay, apoptosis assay and sphere formation assay to analyze the effect of MRK003 on nine patient-derived GICs. Results of these assays demonstrated that MRK003 suppresses GICs viability and sphere formation, and promotes their apoptosis. Nine GICs was classified into relatively sensitive GICs and relatively resistant GICs. Forced expression of the active form of Akt in MRK003-treated relatively sensitive GICs partially rescued the phenotype caused by MRK003, indicating that the mechanism of action is partially mediated through the Akt pathway. Relatively sensitive GICs expressed high-CD44 and low-CD133. In summary, these data indicate that MRK003 may exhibit significant therapeutic potential for GBM harboring GICs with CD44-high and CD133-low expression.

Materials and methods

GBM patient-derived cell culture and transfection

GBM cells used in this study were GICs derived from GBM surgical specimens. Diagnosis was based on the World Health Organization classification [3]. Seven GICs (30R, 1123M, Me83, MD13, 528P, 157NS, and 146NS) were established from freshly resected GBM sample of consenting patients in the Department of Neurological Surgery at The Ohio State University [31–34]. TGS01 and TGS04 GIC were isolated from surgically removed GBM tissues at the University of Tokyo (by TT and YI) [35]. All GBM cells already have been confirmed as tumor-initiating cells since cultured GBM cells have the ability to self-renewal in vitro and mimic the original tumor after intracranial transplantation into immunocompromised mice [31–34]. All patient materials and protocols in this study were approved by the ethics committees of Kanazawa University, the Ohio State University and the University of Tokyo. These GBM-derived neurospheres were cultured as described previously [6, 36, 37].

Vector

Recombinant pcDNA vectors carrying the constitutive, active myristoylated allele of Akt were used for transfection into 30R and 1123M by Nucleofector Kit (Lonza, Basel, Switzerland) by following the company's protocol.

Compounds

The stock solutions of MRK003 (Merck & Co., Inc.; Whitehouse Station, NJ) were dissolved in DMSO at a concentration of 10 mM. The specificity of MRK003 as a γ-secretase inhibitor has been confirmed by us and other investigators [22–25, 27].

Viability assay

Cell viability assay was performed with Cell counting kit-8 (DOJINDO, Kumamoto, Japan) by following the company's protocol. Briefly, all the GBM spheres were dissociated into single cell suspensions by StemPro Accutase (Gibco/Life Technologies). These dissociated GICs were seeded at a density of 1×10^3 cells/100 μl per well into a 96-well Coaster ultra-low attachment plate (Corning, NY) with either MRK003 or DMSO control for 72 h. IC_{50} for MRK003 of each was calculated from non-linear curve fit graph using Graph pad prism 5 (Graph Pad Software, Inc., San Diego).

Apoptosis assay

Apoptosis assay was performed using the Annexin V-FITC detection kit as per the manufacturer's protocol (BD Pharmingen, San Diego, CA). GICs were seeded at a density of 1×10^5 cells/2 ml/well in a 6-well plate in neurosphere medium with MRK003 or DMSO control.

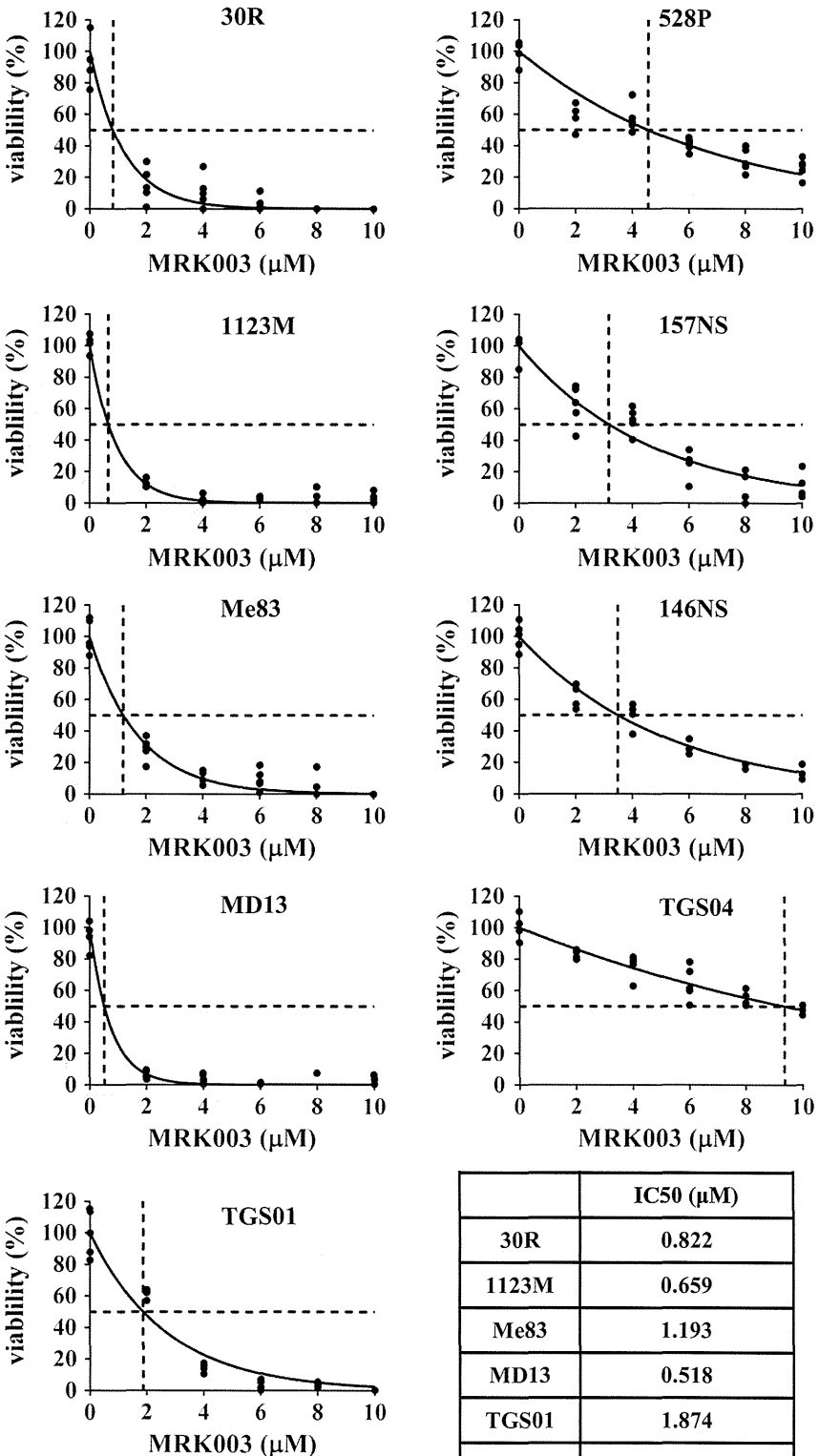

	IC50 (μM)
30R	0.822
1123M	0.659
Me83	1.193
MD13	0.518
TGS01	1.874
528P	4.563
157NS	3.17
146NS	3.48
TGS04	9.371

Fig. 1 MRK003 inhibited viability of nine GICs derived from patients in a dose-dependent manner. 30R, 1123M, MD13, Me83 and TGS01 were relatively sensitive for MRK003. 528P, 157NS, 146NS and TGS04 were relatively resistant for MRK003. Experiments were performed three times. Each data shown were representative. IC_{50} was X-value of intersection of non-linear fitting *graph line* with 50 % viability dotted line

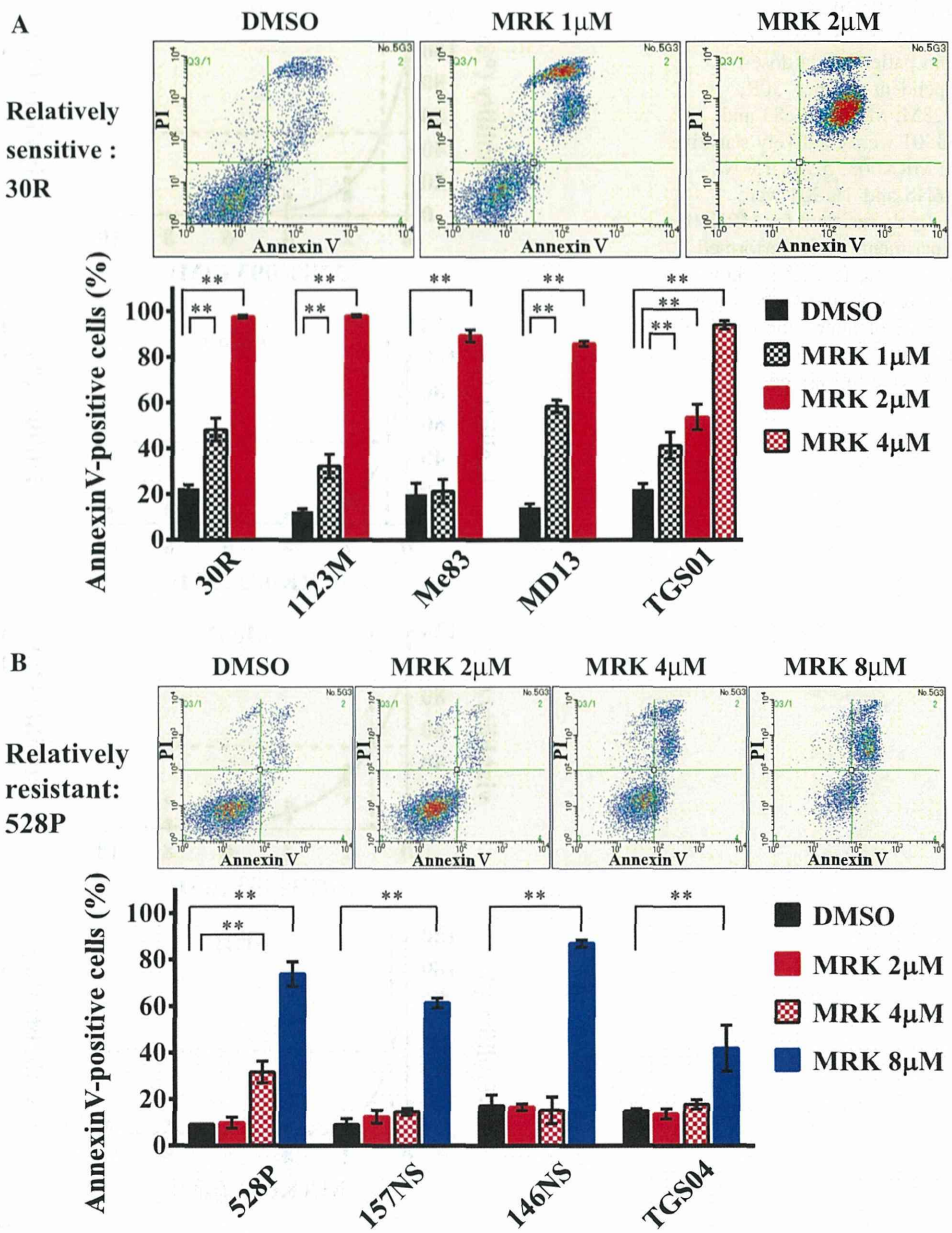

Fig. 2 MRK003 induced apoptosis in GICs. **a** MRK003 relatively sensitive GICs exhibited dramatically increased apoptosis percentage with 2 or 4 μM MRK003 compared with DMSO control. **b** 528P GIC exhibited significantly increased percentage of Annexin V-positive cells with 4 μM MRK003. In 157NS, 146NS, and TGS04 GICs, Annexin V-positive cell percentages were significantly increased in 8 μM MRK003, compared with DMSO. Representative data of flow cytometry for each GIC were shown. X-axis was indicated as Annexin V-FITC. Y-axis was indicated as PI. Experiments were conducted three times, $n = 3$. $^{*}P < 0.05$, $^{**}P < 0.01$ using 1-way ANOVA

GICs were treated for 72 h. Annexin V-FITC and propidium iodide (PI) double-positive cells and only Annexin V-FITC positive cells were measured by flow cytometry (JSAN; Bay bioscience Inc., Kobe, Japan).

Tumorsphere-forming assay

Sphere forming assay was performed as described previously [36, 37]. Briefly, the cultured GICs were dissociated with Stempro Accutase. The dissociated in single-cell suspension (5×10^2 cells/200 μl) were seeded in 96-well Coaster Ultra-low attachment plate in 1.0 % methylcellulose neurosphere medium with MRK003 or DMSO (control). After incubation for 7 days, tumorsphere was counted and tumorsphere-diameter was measured.

Western blot

GICs were treated with DMSO or MRK003 for 48 h and then lysed in a buffer containing 100 mM Tris (pH 6.7), 4 % SDS, phosphatase inhibitor (Thermo Fisher Scientific Inc., Waltham, MA) and protease inhibitors (complete mini) (Roche Applied Science, Indianapolis, IN). Western blotting was performed as previously [36, 37]. The following antibodies were used; total Akt, phospho-Akt (Ser473) (1:1,000 dilution, Cell Signaling Technology,

Danvers, MA) and β-actin (1:100,000 dilution, Sigma-Aldrich, St. Louis, MO).

Fluorescence activated cell sorting (FACS) for CD44/CD133 analysis

GICs were dissociated into single cells and stained with FITC-conjugated human CD44 antibody (BD Biosciences, San Jose, CA, USA) and PE-conjugated human CD133/2 antibody (Miltenyi Biotec, Bergisch Gladbach, Germany). FITC mouse IgG2b isotype (BD Biosciences) and PE mouse IgG2b isotype (Miltenyi Biotec) were used as control antibodies. The stained GICs were analyzed by flow cytometry.

Statistical analysis

All values were expressed as mean ± SD. Statistical analyses were done using Graph Pad Prism 5 software. Comparisons were drawn using 1-way ANOVA or 2-way ANOVA, followed by the Bonferroni post hoc test. The correlativity between expression of CD44-FITC or CD133-

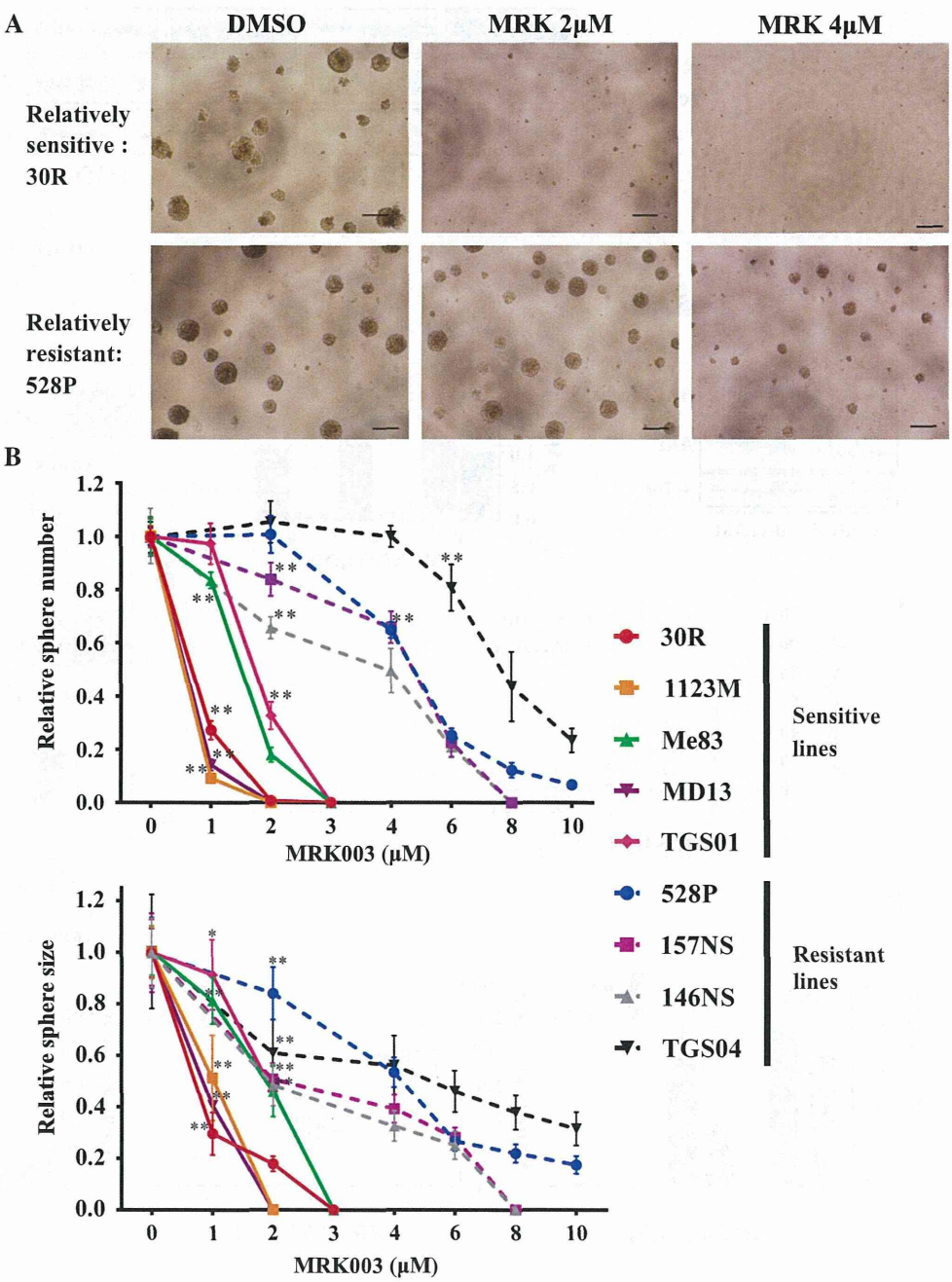

Fig. 3 MRK003 suppressed sphere-forming ability of GICs. **a** Micrographs showed the representative tumorsphere of relatively sensitive 30R and relatively resistant 528P after 7 days of MRK003 treatment. *Scale bar*, 200 μm. **b** The sphere number and size of *sensitive lines* were dramatically decreased in 1 or 2 μM MRK003. *Sphere* number of *resistant lines* was strongly decreased in more than 4 μM MRK003. Both 157NS and 146NS sphere were diminished in 8 μM MRK003. *Sphere-size* of resistant lines was significantly reduced in a dose-dependent manner from 2 μM MRK003. Experiments were conducted three times. $^{*}P < 0.05$, $^{**}P < 0.01$, using one-way ANOVA